View metadata, citation and similar papers at core.ac.uk
brought to you by CORE
provided by E-space: Manchester Metropolitan University's Research Repository

Threshold and Scaling Factor Optimization for Enhancing Impulsive Noise Cancellation in PLC Systems

Khaled M. Rabie and Emad Alsusa
Microwave and Communication Systems (MACS) Group,
School of Electrical and Electronic Engineering,
The University of Manchester, United Kingdom, M13 9PL,
Emails: {khaled.rabie@manchester.ac.uk; e.alsusa@manchester.ac.uk}

***Abstract*—Power-line communication (PLC) is considered as the backbone of smart grid. Impulsive noise (IN) over such channels, however, remains the main factor responsible for degrading communication signals. A simple method to mitigate IN over PLC channels is to precede the receiver with a nonlinear preprocessor to blank and/or clip the incoming signal when it exceeds a certain threshold. Applying a combination of blanking and clipping in a hybrid fashion was shown to provide the best performance. The hybrid scheme is characterized by two thresholds T_1 and T_2 $(T_1 = \alpha T_2)$, where α is a scaling factor. Previous studies assume a fixed value for the scaling factor and found that optimizing the threshold T_2 is the key to enhance performance. In this paper, we show that the performance of this scheme is sensitive not only to the threshold, but also to the scaling factor. With this in mind, a mathematical expression for the output signal-to-noise ratio as a function of the threshold and scaling factor is formulated and used to optimize the hybrid scheme performance. Simulation results are also provided to validate our analysis. The results reveal that using an adaptive hybrid scheme with an optimally selected threshold and scaling factor always outperforms other nonlinear schemes.**

***Index Terms*—Blanking, clipping, hybrid, impulsive noise, power-line communications (PLC), signal-to-noise ratio (SNR), smart grids.**

I. Introduction

SMART Grids, after the invention of the internet, are the next big technological revolution and have been one of the most growing fields of research recently. Smart grids are expected to be a crucial factor in shaping tomorrow's societies and can be attained via different technologies such as wireless, coaxial or power-line communications (PLC) [1]. PLC, however, has been the most attractive for several reasons. For instance, the pre-installed infrastructure of wiring networks and the availability of power outlets in every room make PLC technology a very attractive alternative for networking applications. The idea of utilizing power-line networks for communication is not new; in fact, the first communication attempt over power-lines was in 1900s for reading meters at remote locations [2] and few decades later, these cables were considered for voice transmission. These technologies used single-carrier narrow-band schemes operating in the low frequency-bands providing data rates in the range of few kilobits per second. Over the recent decades, the rising dependence on communications has increased dramatically and because of the advances in communication, modulation techniques as well as signal processing, it has become possible to deploy power-lines for high-speed communication with data rates comparable to that provided by wired networks and wireless LANs [3]–[5].

Power-lines are not well suited for communication signals since they have not been designed for such purposes. Thus, in order to improve the reliability of PLC, several inherent challenges must be overcome such as the varying impedance of the wiring, high levels of frequency-dependent attenuation [6], [7] and the noise. Noise over power-lines is classified into background noise (BN) and impulsive noise (IN) [8]–[10]. The latter, however, is the most dominant factor degrading communication signals and its power spectral density (PSD) always exceeds the PSD of the BN by at least $10-15$ dB and may reach as much as 50 dB [11]. To analyze and evaluate the system performance over IN channels, the two-component mixture-Gaussian noise model, [12], [13], has been widely accepted and, therefore, it will be adopted in this paper.

A number of methods have been introduced in the literature with different degrees of complexity to reduce the noxious effect of IN; the simplest and most efficient of which is the application of nonlinear devices at the receiver front-end such as blanking, clipping or hybrid (joint blanking and clipping) to blank or/and clip the received signal when it exceeds certain thresholds [13]–[17]. This method is widely used in practice because of its simplicity and ease of implementation. It is presented in [14] that the hybrid scheme provides better performance compared to the other nonlinear methods. In this scheme two thresholds are set T_1 and T_2 to clip or blank the incoming signal when it exceeds these thresholds, respectively. These thresholds are related by the scaling factor (α) as $T_1 = \alpha T_2$. So far, all work on this topic assumes a fixed scaling factor. This method will be referred to here as the conventional hybrid method.

In contrast, in this paper, we show that the hybrid scheme is not only sensitive to the threshold but also to the scaling factor. Then the problem of threshold and scaling factor optimization is analyzed mathematically and the corresponding maximum achievable output signal-to-noise ratio (SNR) is presented. In addition, simulation results are provided to corroborate our analysis. The results show that the adaptive scheme can

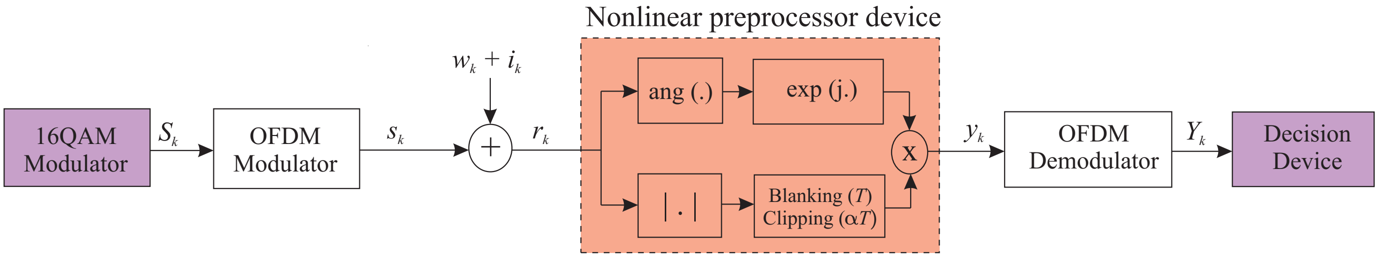

Figure 1: System diagram with nonlinear preprocessors at the receiver

provide up to 0.6 dB enhancement in the output SNR relative to the conventional hybrid scheme.

The rest of the paper is organized as follows. In Section II, the system model is described. In Section III, the output SNR is analyzed and the problem of threshold and scaling factor optimization is addressed. Some numerical and simulation results are outlined in Section IV. Finally, conclusions are drawn in Section V.

II. System Model

The basic system model used in this study is illustrated in Fig. 1. First, the information bits are mapped into 16 quadrature amplitude modulation (16-QAM) base band symbols S_k. Then, these symbols are passed through an orthogonal frequency division multiplexing (OFDM) modulator to produce a time domain signal

$$s(t) = \frac{1}{\sqrt{N}} \sum_{k=0}^{N-1} S_k e^{\frac{j2\pi kt}{T_s}}, \quad 0 < t < T_s \tag{1}$$

where S_k is the complex constellations of the data symbols, N is the number of sub-carriers and T_s is the active symbol interval.

As mentioned previously, in this work the two-component mixture-Gaussian noise model is used in which IN is modeled as a Bernoulli-Gaussian random process given by [12]

$$n_k = w_k + i_k \quad k = 0, 1, 2, \ldots, N-1 \tag{2}$$

where

$$i_k = b_k \, g_k, \quad k = 0, 1, 2, \ldots, N-1 \tag{3}$$

n_k is the total noise component, w_k is the additive white Gaussian noise (AWGN), i_k is the IN, g_k is complex white Gaussian noise with mean zero and b_k is the Bernoulli process with probability mass function

$$\Pr(b_k) = \begin{cases} p, & b_k = 1 \\ 0, & b_k = 0 \end{cases} \quad k = 0, 1, \ldots, N-1 \tag{4}$$

where p denotes the IN probability of occurrence. The probability density function (PDF) of the total noise can be expressed as

$$P_{n_k}(n_k) = p_0 \, \mathcal{G}\left(n_k, 0, \sigma_0^2\right) + p_1 \, \mathcal{G}\left(n_k, 0, \sigma_1^2\right) \tag{5}$$

$\mathcal{G}(.)$ is the Gaussian PDF given by (6), $p_0 = (1-p)$, $p_1 = p$, $\sigma_0^2 = \sigma_w^2$ and $\sigma_1^2 = \sigma_w^2 + \sigma_i^2$. The variances σ_w^2 and σ_i^2 denote the AWGN and IN power and define the input SNR and signal-to-impulsive noise ratio (SINR) as in (7) and (8), respectively.

$$\mathcal{G}\left(x, \mu, \sigma_x^2\right) = \frac{1}{\sqrt{2\pi\sigma_x^2}} e^{-\frac{(x-\mu)^2}{2\sigma_x^2}} \tag{6}$$

$$\mathrm{SNR} = 10 \log_{10}\left(\frac{\sigma_s^2}{\sigma_w^2}\right) \tag{7}$$

$$\mathrm{SINR} = 10 \log_{10}\left(\frac{\sigma_s^2}{\sigma_i^2}\right) \tag{8}$$

where σ_s^2 is the transmitted signal variance. Under perfect synchronization condition, the received signal is defined as

$$r_k = s_k + w_k + i_k, \quad k = 0, 1, 2, \ldots, N-1 \tag{9}$$

while $s_k = s\left(kT_s/N\right)$; s_k, w_k and i_k are assumed to be mutually independent. In order to reduce the effect of IN, one of the following nonlinear preprocessors is applied at the front-end of the receiver

- Blanking

$$y_k = \begin{cases} r_k, & |r_k| \le T_1 \\ 0, & |r_k| > T_1 \end{cases} \quad k = 0, 1, \ldots, N-1 \tag{12}$$

  where T_1 is the blanking threshold.
- Clipping

$$y_k = \begin{cases} r_k, & |r_k| \le T_2 \\ T_2 \, e^{j \arg(r_k)}, & |r_k| > T_2 \end{cases} \quad k = 0, 1, \ldots, N-1 \tag{13}$$

  where T_2 is the clipping threshold.
- Conventional Hybrid

$$y_k = \begin{cases} r_k, & |r_k| \le T_2 \\ T_2 \, e^{j \arg(r_k)}, & T_2 < |r_k| \le T_1 \\ 0, & |r_k| > T_1 \end{cases} \quad k = 0, 1, \ldots, N-1 \tag{14}$$

  where $T_1 = 1.4 \, T_2$.

$$K_o = 1 - \sum_{i\epsilon\{0,1\}} p_i \left[e^{-\frac{T^2}{2(1+\sigma_i^2)}} + \frac{T^2}{2\left(1+\sigma_i^2\right)} e^{-\frac{\alpha^2 T^2}{2(1+\sigma_i^2)}} \right] - \sum_{i\epsilon\{0,1\}} p_i \sqrt{\frac{\pi}{2}} \frac{T}{\sqrt{1+\sigma_i^2}} \left[Q\left(\frac{T}{\sqrt{1+\sigma_i^2}}\right) - Q\left(\frac{\alpha T}{\sqrt{1+\sigma_i^2}}\right) \right] \quad (10)$$

$$E_{out} = 2 + 2 \sum_{i\epsilon\{0,1\}} p_i \left(\sigma_i^2 - \left(1+\sigma_i^2\right) e^{-\frac{T^2}{2(1+\sigma_i^2)}} - \frac{T^2}{2} e^{-\frac{\alpha^2 T^2}{2(1+\sigma_i^2)}} \right) \quad (11)$$

- Adaptive Hybrid

$$y_k = \begin{cases} r_k, & |r_k| \leq T \\ \alpha T\, e^{j\arg(r_k)}, & T < |r_k| \leq \alpha T \quad k = 0, 1, \ldots, N - \\ 0, & |r_k| > T \end{cases} \quad (15)$$

where r_k and y_k are the input and the output of the nonlinear devices, respectively, and $\alpha > 1$. It is clear that these devices only process the amplitude of the received signal leaving its phase unmodified. The threshold(s) or (the threshold and the scaling factor in case of adaptive hybrid) should be carefully selected to optimize the system performance. For instance, if the resulting threshold is too small, many unaffected samples of the OFDM signal will be blanked resulting in poor bit error rate performance; whereas for very large threshold, IN will be overlooked and will become part of the detected signal; hence will degrade performance.

III. Performance Analysis

In this section we analyze the SNR at the output of the adaptive hybrid device and optimize the threshold and the scaling factor to maximize the system performance.

A. Output SNR

The SNR performance at the output of the adaptive hybrid scheme is investigated here. For the four types of nonlinear preprocessors (12), (13), (14) and (15), the output SNR can be expressed as [14]

$$\text{SNR}_{out} = \frac{2K_o^2}{E_{out} - 2K_o^2} \quad (16)$$

where K_o is a real constant and E_{out} is the total signal power at the output of the nonlinear preprocessor. These parameters are derived in [14] for the blanking, clipping and conventional hybrid methods. For the adaptive hybrid scheme, K_o and E_{out} are found by replacing $T_1 \to T$ and $T_2 \to \alpha T$ of [14, Eq. (19)] and [14, Eq. (21)] to yield (10) and (11). To illustrate the impact of the threshold T and the scaling factor α on the output SNR of the proposed scheme, some numerical results are presented in Fig. 2. This figure shows a surface plot of the output SNR as a function of T and α. These results are obtained from (16) for SNR $=$ 25 dB, SINR $= -15$ dB and $p = 0.01$. In general, there is a general trend that when T and α are too small $\{T \lesssim 2 \text{ and } \alpha \lesssim 3\}$ the system performance degrades significantly due to the significant loss of the useful signal energy. On the other hand, when T and α are too high $\{T \to \infty \text{ and } \alpha \to \infty\}$, i.e. no blanking/clipping is performed (typical OFDM receiver), this allows all the IN energy to be part of the detected signal and will eventually cause dramatic performance deterioration. In such a scenario, the output SNR approaches -10 dB as illustrated in Fig. 2. This can be mathematically expressed as (17)

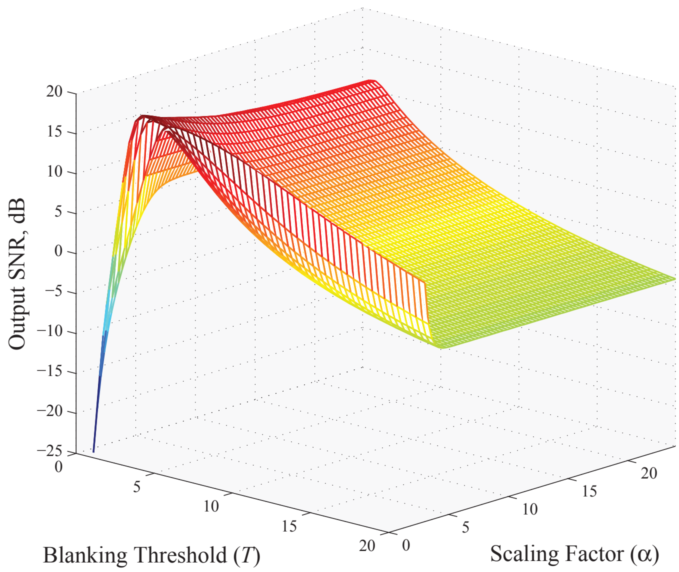

Figure 2: Surface plot of the SNR at the output of the adaptive hybrid device as a function of the blanking threshold and the scaling factor for SINR $= -15$ dB, $p = 0.01$ and SNR $= 25$ dB.

$$\text{SNR}_{\text{out}}\left(T \to \infty,\, \alpha \to \infty,\right) = 10\log_{10}\left(\frac{\sigma_s^2}{\sigma_w^2 + p\,\sigma_i^2}\right) \quad (17)$$

when $p\,\sigma_i^2 \gg \sigma_w^2$, (17) can be approximated to

$$\simeq 10\log_{10}\left(\frac{1}{p\,\sigma_i^2}\right) \quad (18)$$

However, it is also interesting to note that for given IN characteristics, good selection of both the threshold and the scaling factor will maximize the output SNR. The problem of optimizing these parameters is investigated next.

B. Threshold and Scaling Factor Optimization

Determining the threshold and the scaling factor is the key for achieving best performance in the adaptive hybrid scheme. To optimize the output SNR it is more convenient to rewrite (16) as

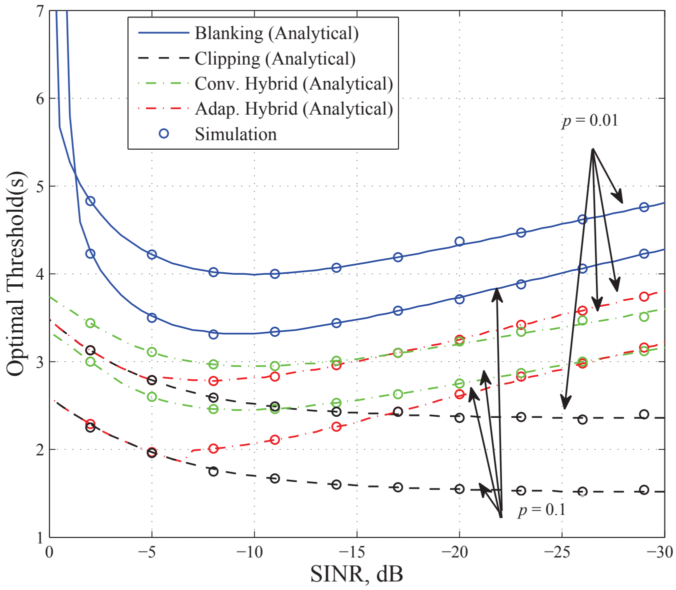

Figure 3: Optimal threshold(s) (with optimized scaling factor) versus SINR for various values of p and SNR $= 25$ dB; simulated results for 16-QAM OFDM with $N = 256$.

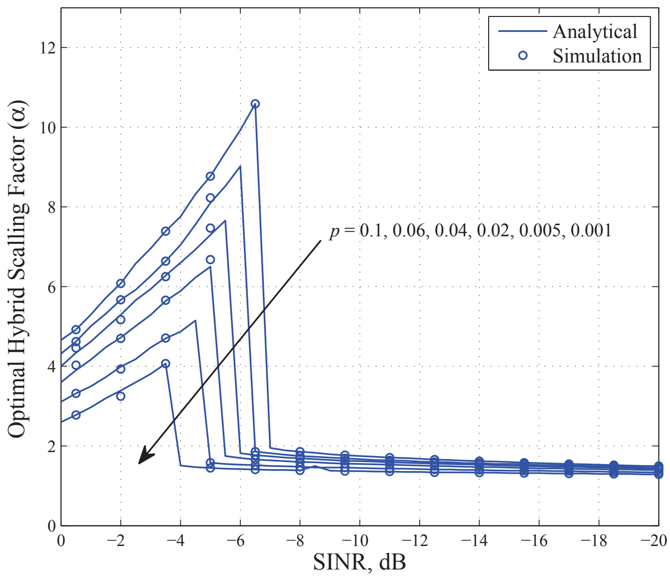

Figure 4: The optimal scaling factor (with optimized threshold T) versus SINR for various values of p and SNR $= 25$ dB; simulated results for 16-QAM OFDM with $N = 256$.

$$(\mathrm{SNR}_{out})^{-1} = \frac{E_{out}}{2K_o^2} - 1 \tag{19}$$

The optimal threshold and optimal scaling factor cannot be expressed in closed forms hence only numerical results can be obtained by satisfying the following argument

$$\underset{T,\,\alpha}{min} \left\{ \frac{E_{out}}{K_o^2} \right\} \tag{20}$$

IV. Numerical and Simulation Results

In this section we present some numerical results for the optimal threshold and the optimal scaling factor that maximize the output SNR. In addition, the corresponding maximum achievable output SNR is investigated under various IN conditions. These analytical results are validated with simulations. The simulation parameters used here are: $N = 256$ sub-carriers, 16-QAM modulation, $\sigma_s^2 = (1/2)\,\mathbb{E}[|s_k|^2] = 1$, $\sigma_w^2 = (1/2)\,\mathbb{E}[|w_k|^2]$, $\sigma_i^2 = (1/2)\,\mathbb{E}[|i_k|^2]$ and the simulated output SNR is found by (21) where K_o is chosen as $K_o = (1/2)\,\mathbb{E}\left[|y_k s_k^*|^2\right]$. Also, in all our investigations we set the input SNR $= 25$ dB.

$$\mathrm{SNR_{out}} = \frac{\mathbb{E}\left[|K_o\, s_k|^2\right]}{\mathbb{E}\left[|y_k - K_o\, s_k|^2\right]} \tag{21}$$

Fig. 3 illustrates some numerical and simulated results of the optimal thresholds for the blanking, clipping, conventional hybrid and adaptive hybrid techniques when α is optimized. Whereas the optimal scaling factor corresponding to the optimized T is plotted versus SINR in Fig. 4 for various IN probabilities. In both figures, it is clearly visible that the analytical and simulated results are in good agreement. The analytical results of the optimal thresholds for the first three techniques are obtained from the expressions derived in [14] whereas for the adaptive technique the results of the optimal threshold and optimal scaling factor are obtained by satisfying (20).

In general, it is obvious that the behavior of the optimal values for T and α for the adaptive system can be divided into two regions during which these parameters behave differently. These regions can be defined as the high SINR region $\{0 \rightarrow -6\,\mathrm{dB}\}$ and low SINR region $\{-6\,\mathrm{dB} \rightarrow -\infty\}$. In the former region, it is interesting to observe that the optimal threshold of the adaptive scheme matches the optimal clipping threshold and this corresponds to the high dependency of the optimal scaling factor on the IN characteristics as shown in Fig. 4. To elaborate, having a large value for α means that the blanking threshold (αT), of the adaptive hybrid system, will be too high and therefore the vast majority of the received samples will not be blanked. As a consequence, clipping becomes the dominant process which justifies why the optimal threshold of the adaptive system approaches the clipping threshold. Moreover, it should be highlighted that the variation in the optimal scaling factor increases as the IN probability of occurrence becomes higher making the selection of this parameter even more crucial in heavily-disturbed IN environments. One the other hand, in the low SINR region it is noticeable that the optimal threshold of the proposed system starts to diverge from the clipping threshold and approaches the threshold of the conventional hybrid system. However, the corresponding optimal scaling factor drops sharply and remains almost constant at about 1.4 which is equal to the scaling factor value of the conventional hybrid technique (14). This clearly explains why the optimal threshold of the adaptive system approaches that of the conventional hybrid technique for very low SINR values.

In order to calculate the maximum achievable SNR at the output of the adaptive hybrid device, the numerically found

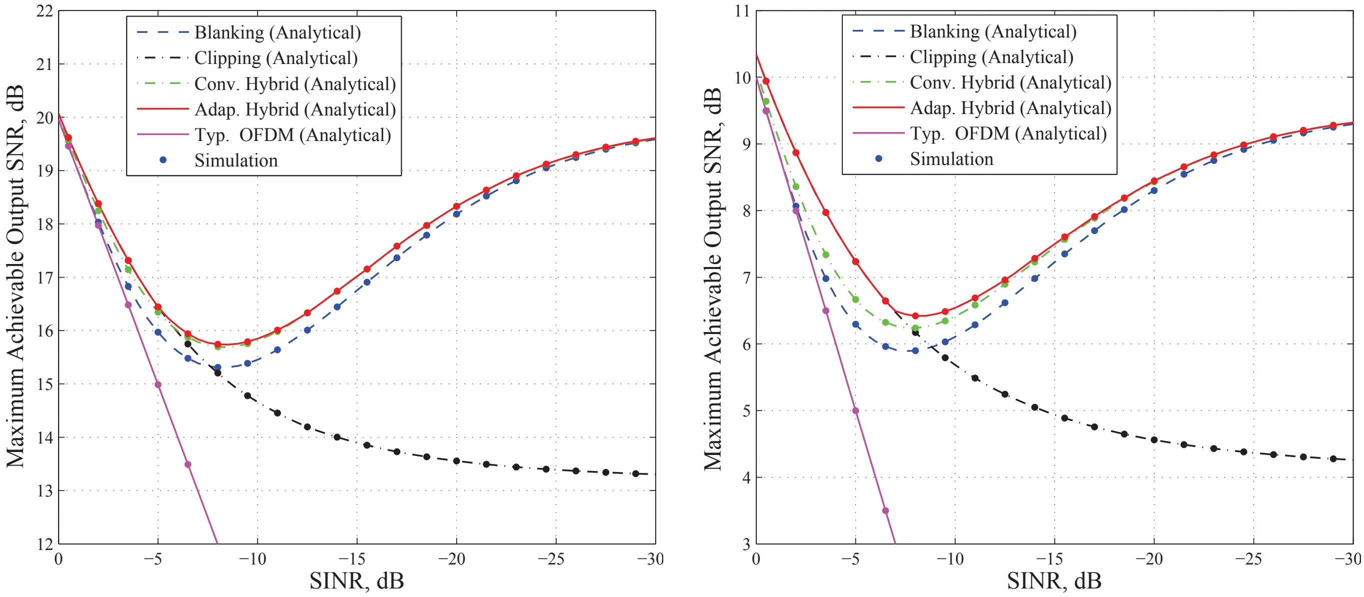

(a) $p = 0.01$ (b) $p = 0.1$

Figure 5: Maximum achievable output SNR versus SINR for the blanking, clipping, conventional hybrid, adaptive hybrid and typical OFDM systems with various IN probabilities when SNR $= 25$ dB.

optimal threshold and optimal scaling factor are substituted in (10), (11) and (16). Fig. 5 depicts the maximum achievable output SNR as a function of SINR for the four nonlinear techniques with different IN probabilities. For the sake of comparison, the output SNR of the typical OFDM receiver (17) is also included on this plot and it is evident that this system has the worst performance especially as IN becomes higher. On the other hand, it is seen that the adaptive technique offers the best performance which can be best quantified in terms of the relative gain. This gain is defined as the gain in the output SNR obtained by the adaptive hybrid technique $\text{SNR}_{\text{out}}^{(AH)}$ over the conventional hybrid technique $\text{SNR}_{\text{out}}^{(CH)}$ (22) and is plotted in Fig. 6 for various values of p.

$$G_R = 10\log_{10}\left(\frac{\text{SNR}_{\text{out}}^{(AH)}}{\text{SNR}_{\text{out}}^{(CH)}}\right) \tag{22}$$

As apparent, the relative gain is directly proportional to p and can be as high as 0.62 dB at about SINR $= -4$ dB when $p = 0.1$. The intuitive explanation of this is that when the IN probability of occurrence is high the decision accuracy of whether to blank or clip becomes more critical and this is where the adaptive hybrid scheme is most effective as it optimizes the blanking/clipping scaling factor which guides the decision process. This can also be extracted from Fig. 4 where the optimal scaling factor variation increases for higher IN probabilities. On the other hand, when the IN probability is low, i.e. $p = 0.001$, the gain becomes negligible and hence the conventional hybrid technique could be applied instead since it is simpler. Furthermore, it is evident that, irrespective of the IN probability, the conventional and adaptive hybrid systems perform similarly when SINR is very low. This can be easily explained as follows: in such an environment the IN amplitude is so high, compared to the OFDM signal, that it can be identified perfectly with either technique. In other words, the decision accuracy of whether to blank or clip will have less influence on the overall performance.

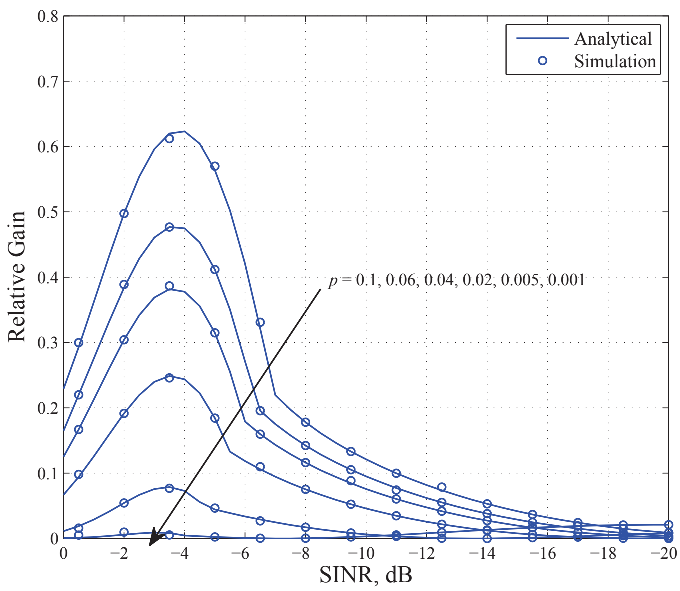

Figure 6: The output SNR gain relative to the conventional hybrid scheme ($T_1 = 1.4T_2$) versus SINR for various values of p, SNR $= 25$ dB; simulated results for 16-QAM OFDM with $N = 256$.

V. Conclusion

IN can significantly deteriorate the communication performance in PLC systems and in order to reduce its effect, blanking, clipping and hybrid nonlinear preprocessors are usually applied at the receiver. In this paper we have proposed to enhance the capability of the hybrid technique (combined blanking and clipping) by jointly optimizing the threshold and the scaling factor to maximize the output SNR. A closed-form expression for the output SNR is found and some numerical results are also obtained for the optimal threshold; in addition, the analytical results have been validated through computer simulations. It was demonstrated that the proposed scheme is able to yield up to 0.6 dB SNR improvement relative to the conventional hybrid system.

References

[1] B. Adebisi, A. Treytl, A. Haidine, A. Portnoy, R. Shan, D. Lund, H. Pille, and B. Honary, "IP-centric high rate narrowband PLC for smart grid applications," *IEEE Commun. Mag.*, vol. 49, no. 12, pp. 46–54, 2011.

[2] M. Schwartz, "Carrier-wave telephony over power lines: Early history [history of communications]," *IEEE Commun. Mag.*, vol. 47, no. 1, pp. 14–18, 2009.

[3] H. Latchman and L. Yonge, "Power line local area networking," *IEEE Commun. Mag.*, vol. 41, no. 4, pp. 32–33, 2003.

[4] N. Pavlidou, A. J. H. Vinck, J. Yazdani, and B. Honary, "Power line communications: state of the art and future trends," *IEEE Commun. Mag.*, vol. 41, no. 4, pp. 34–40, 2003.

[5] S. Galli, A. Scaglione, and K. Dostert, "Broadband is power: internet access through the power line network," *IEEE Commun. Mag.*, vol. 41, no. 5, pp. 82–83, 2003.

[6] D. Anastasiadou and T. Antonakopoulos, "Multipath characterization of indoor power-line networks," *IEEE Trans. Power Del.*, vol. 20, no. 1, pp. 90–99, Jan. 2005.

[7] M. Zimmermann and K. Dostert, "A multipath model for the powerline channel," *IEEE Trans. on Commun.*, vol. 50, no. 4, pp. 553–559, 2002.

[8] D. Middleton, "Canonical and quasi-canonical probability models of class a interference," *IEEE Trans. Electromagn. Compat.*, vol. EMC-25, pp. 76–106, May 1983.

[9] ——, "Non-gaussian noise models in signal processing for telecommunications: new methods an results for class A and class B noise models," *IEEE Trans. Inform. Theory*, vol. 45, no. 4, pp. 1129 –1149, May 1999.

[10] M. G. Sanchez, L. de Haro, M. C. Ramon, A. Mansilla, C. M. Ortega, and D. Oliver, "Impulsive noise measurements and characterization in a UHF digital TV channel," *IEEE Trans. Electromagn. Compat.*, vol. 41, no. 2, pp. 124 –136, May 1999.

[11] M. Zimmermann and K. Dostert, "Analysis and modeling of impulsive noise in broad-band powerline communications," *IEEE Trans. Electromagn. Compat.*, vol. 44, pp. 249–258, Feb. 2002.

[12] M. Ghosh, "Analysis of the effect of impulse noise on multicarrier and single carrier QAM systems," *IEEE Trans. Commun.*, vol. 44, no. 2, pp. 145–147, Feb. 1996.

[13] S. V. Zhidkov, "Performance analysis and optimization of OFDM receiver with blanking nonlinearity in impulsive noise environment," *IEEE Trans. Veh. Technol.*, vol. 55, no. 1, pp. 234–242, Jan. 2006.

[14] ——, "Analysis and comparison of several simple impulsive noise mitigation schemes for ofdm receivers," *IEEE Trans. commun.*, vol. 56, no. 1, pp. 5–9, Jan. 2008.

[15] E. Alsusa and K. Rabie, "Dynamic peak-based threshold estimation method for mitigating impulsive noise in power-line communication systems," *IEEE Trans. Power Del.*, vol. 28, no. 4, pp. 2201–2208, Oct. 2013.

[16] K. Rabie and E. Alsusa, "Quantized peak based impulsive noise blanking in power-line communications," *IEEE Trans. Power Del.*, 2013, Accepted.

[17] ——, "Preprocessing based impulsive noise reduction for power-line communications," *IEEE Trans. Power Del.*, 2014, Accepted.